Available online at www.sciencedirect.com
SCIENCE DIRECT®
European Journal of Pharmaceutics and Biopharmaceutics 63 (2006) 249–261
European Journal of Pharmaceutics and Biopharmaceutics
www.elsevier.com/locate/ejpb

Research paper

Controlled release of cephalexin through gellan gum beads: Effect of formulation parameters on entrapment efficiency, size, and drug release ☆,☆☆

Sunil A. Agnihotri, Sheetal S. Jawalkar, Tejraj M. Aminabhavi *

Drug Delivery Division, Center of Excellence in Polymer Science, Karnatak University, Dharwad, India

Received 17 January 2005; accepted in revised form 15 December 2005
Available online 6 March 2006

Abstract

Gellan gum beads containing cephalexin were prepared by extruding the dispersion of cephalexin and gellan gum into a solution containing a mixture of calcium and zinc ions (counterions). Beads were prepared by changing experimental variables such as pH of the counterion solution and amount of cephalexin loading in order to optimize process variables on the final % drug entrapment efficiency, release rates, size, and morphology of the beads. Absence of chemical interactions between drug, anionic polymer, and counterions after production of beads was confirmed by Fourier transform infrared spectroscopy. Differential scanning calorimetry was used to understand the crystalline nature of the drug after its successful entrapment. These data indicated the amorphous dispersion of cephalexin in the polymer matrix. Beads were spherical in shape, with the average bead size ranging from 925 to 1183 μm as measured by the laser light scattering technique. Cephalexin entrapment of up to 69.24% was achieved. In vitro release studies were performed in 0.1 N HCl or pH 7.4 phosphate buffer and the release of cephalexin was achieved up to 6 h. Dynamic swelling studies were performed in 0.1 N HCl or pH 7.4 phosphate buffer. Diffusion coefficients were calculated for spherical geometry. The release data have been fitted to an empirical relation to estimate the transport parameters. Mathematical modeling studies were performed for spherical geometry by solving Fick's equation to compute concentration profiles. These results were correlated with the release profiles.

Keywords: Gellan gum; Beads; Cephalexin; Controlled release; Modeling

1. Introduction

Over the past decades, hydrogel polymers have attracted a great deal of attention for use as potential carriers in controlled and site-specific delivery of drugs [1–4]. Hydrogels are the hydrophilic, three-dimensional network structures having the natural propensity to absorb large quantity of water or biological fluids and they resemble those of biological tissues. The ability of hydrogels to swell in the presence of water or biological fluids regulates the release of the encapsulated drugs. By controlling the degree of swelling due to crosslinking makes them potential carriers of drugs for controlled release (CR) applications [5–7]. Recently, we have been actively involved in the development of hydrogel-based CR formulations for the delivery of a variety of bioactive agents [8–11]. In view of their greater advantages than the synthetic polymers, the biocompatible polymers such as chitosan, sodium alginate, guar gum, etc. have been widely used in the literature of pharmaceutics. However, to control the release patterns, many attempts have been made to use the synthetically modified natural polymers such as polyacrylamide-*g*-guar gum, etc. [11]. In continuation of our earlier reports on the use of hydrogels as CR systems and as part of our ongoing program of research, we now present experimental data on use of gellan gum

☆ Part of this paper was presented at the 31st International Symposium on Controlled Release of Bioactive Materials, Honolulu, Hawaii, USA, June 2004.
☆☆ This paper is CEPS Communication # 43.
* Corresponding author. Tel.: +91 836 2779983; fax: +91 836 2771275.
E-mail address: aminabhavi@yahoo.com (T.M. Aminabhavi).

0939-6411/$ - see front matter © 2006 Elsevier B.V. All rights reserved.
doi:10.1016/j.ejpb.2005.12.008

(GG) as a matrix material to investigate the CR of cephalexin, a broad spectrum bactericidal antibiotic. It is almost completely absorbed from the gastrointestinal tract, its plasma half-life is about 1 h, and more than 80% of the dose is excreted unchanged in the urine during the first 6 h. In an earlier report [12], a granule form of the sustained release cephalexin (L-Keflex) was evaluated for safety and efficacy by comparing it with Keflex (capsule of regular cephalexin). It was judged that L-Keflex (granule) had better patient convenience than Keflex (capsule) in that it can be administered with twice daily regimen. However, there are no other reports on the formulations of cephalexin as CR particulate drug delivery systems. The specific advantages of the particulate drug delivery systems have been discussed earlier [13]. Since the use of CR formulations offers many potential advantages like sustained blood levels, attenuation of adverse effects, and improved patient compliance, it is realized that in case of antibiotics with short half-life, it is necessary to maintain the constant blood levels as otherwise microorganisms will become resistant to the antibiotic. Therefore, formulating cephalexin in CR dosage forms will increase the therapeutic efficacy and patient compliance.

GG used in this study is a linear anionic polysaccharide obtained from exocellular secretion of the microorganism, *Pseudomonas elodea* [14]. The natural form of GG is composed of the linear structure of a repeating tetrasaccharide unit of glucose, glucuronic acid, and rhamnose in a molar ratio of 2:1:1 [15]. It is partially acetylated with acetyl and L-glyceryl groups located on the glucose residues [16]. However, the presence of acetyl groups interferes in ion bonding ability. On the other hand, the commercially available GG is a deacetylated product obtained by treatment with alkali [14]. Because of the presence of free carboxylate groups in GG, it becomes anionic in nature and thus, would possess the characteristic property of undergoing ionic gelation in the presence of mono- and divalent cations. However, the affinity for divalent cations is much stronger than the monovalent cations [17]. The mechanism of gelation involves the formation of double helical junction zones followed by aggregation of double helical segments to form a three-dimensional network by complexation with cations and hydrogen bonding with water [18]. GG has a wide variety of applications mainly in food and pharmaceutical industries. In view of the characteristic property of cation-induced gelation, it has been widely used in the formulation of in situ gelling ophthalmic preparations [19,20] as well as in situ gelling oral sustained release formulations [21–23]. Quigley and Deasy [24] developed the sustained release beads containing GG for the CR of sulfamethizole prepared by the hot extrusion method into the chilled ethyl acetate. The GG beads containing salbutamol sulfate have also been studied for sustained release applications [25]. Recently, Kedzierewicz et al. [26] have developed the GG beads for the CR of propranolol hydrochloride and found that the drug release was rapid. However, the ionotropic gelation with GG offers new opportunities in the field of bioencapsulation.

Chan et al. [27] recently reported that a combination of calcium and zinc ions could produce more sustained release of drugs from the alginate microspheres compared to calcium ions alone. In the earlier literature, no CR formulations of GG beads containing cephalexin have been studied. This prompted us to develop GG beads containing cephalexin by a rather simple procedure using cation-induced gelation of GG. In this work, we have used the combination of calcium and zinc ions to induce cationic gelation of GG. Various formulation and process variables affecting the preparation of beads and in vitro release characteristics of cephalexin were investigated. The drug-loaded beads were characterized by differential scanning calorimetry (DSC). The Fourier transform infrared (FTIR) spectroscopy was used to study the drug–polymer interactions. Morphology of the formulated beads was investigated by scanning electron microscopy (SEM). The swelling and deswelling kinetics of GG beads were studied to understand their suitability in oral dosage formulations. The drug release data were analyzed in terms of an empirical equation proposed by Ritger and Peppas [28]. Furthermore, diffusion coefficients were computed from the modified Fick's equation. Diffusion data were discussed in terms of the concentration profiles calculated from a numerical scheme [29] to understand the transport of drug/liquid through the spherical beads.

2. Materials and methods

2.1. Materials

The gift samples of cephalexin and deacetylated gellan gum (Gelrite®) (Merck and Co., Inc., NJ, USA) were kindly supplied by Eros Pharma Ltd., Bangalore, India. Analytical reagent grade samples of calcium chloride, zinc sulfate, conc. HCl, and ethylamine were purchased from S.D. Fine-Chemicals, Mumbai, India. Double-distilled water was used throughout the work and all the chemicals were used without further purification.

2.2. Methods

2.2.1. Preparation of beads

Beads were prepared by the cation-induced ionotropic gelation method. A 1.5% (w/v) GG solution was prepared in double-distilled water with constant stirring (300 rpm) at 55 °C. After cooling, the appropriate quantity of cephalexin (25%, 50%, 75% or 100% of the dry mass of GG) was added and stirred until a homogeneous solution was formed. The homogeneous bubble-free solution was extruded dropwise into the counterion solution containing a mixture of 1% calcium chloride and 1% zinc sulfate adjusted to different pH values (5, 7, and 9) using a 25 mL hypodermic syringe (1 mm diameter) with constant stirring. The concentration of counterion solution was cho-

sen based on the earlier report [26]. The beads were formed immediately; after 2 min, the beads were separated by filtration, washed with double-distilled water, and dried in an oven at 37 °C. Formulations were prepared in triplicate and used for further studies. Totally, 12 formulations were prepared and the assigned formulation codes are given in Table 1.

To study the influence of pH of counterion media, pH was adjusted to acidic (pH 5), neutral (pH 7), and basic (pH 9) conditions. To optimize the gelation time of the beads and also to choose the acid or base to adjust the pH of the counterion media, some preliminary experiments were performed. The pH of the counterion media (mixture of 1% calcium chloride and 1% zinc sulfate in distilled water) was slightly acidic (pH about 6.5). For adjusting the pH of the counterion media to 7 or 9, initially 5 N NaOH was used, which resulted in the precipitation of calcium chloride in the form of calcium hydroxide. Instead, 10% ethylamine solution was found to be more useful. On the other hand, counterion medium pH was adjusted to 5 by using 5 N HCl. For the gelation time, beads were removed from the counterion media at 30 s intervals and allowed to dry. Samples removed before the lapse of 2 min have failed to give the perfect spherical structure, possibly due to lack of mechanical strength. Based on this, 2 min exposure time to counterion media was chosen.

2.2.2. Measurement of bead size

Bead size was measured by using a laser light scattering technique (Mastersizer 2000, Malvern, UK). Methanol was used to disperse the GG beads, since GG is insoluble in methanol as confirmed by the preliminary experiments. Completely dried beads of different formulations were dispersed in 100 mL methanol by sonicating for about 1 min. High turbulence was created by circulating methanol to keep the particles separated and properly distributed into methanol medium. After measurement of particle size of each sample, the wet sample adapter was cleaned thoroughly and dried with methanol to avoid any cross contamination. The volume-mean diameter (V_d) was recorded on multiple batches of the bead samples.

2.2.3. Dynamic swelling studies

Dynamic swelling of GG beads was studied in 0.1 N HCl (ionic strength 0.1) and pH 7.4 phosphate buffer (0.05 M potassium dihydrogen phosphate) (ionic strength 0.09) by mass measurements. Beads (≅2 g) were soaked in either 0.1 N HCl or pH 7.4 phosphate buffer media maintained at 37 °C. At different time intervals, few beads representative of the batch consisting of beads with narrow size distribution having an average bead size ranging from 925 to 1183 μm were taken out and blotted carefully with tissue papers (without pressing hard) to remove the surface-adhered liquid droplets. The swollen beads were then weighed (w_1) on an electronic microbalance (Mettler, AE 240, Switzerland) to an accuracy of ±0.01 mg. Beads were then dried in the same container until the attainment of constant mass (w_2) in an oven maintained at 60 °C. Usually, the drying process lasted up to 5 h. These studies were performed in triplicate for each set of formulated samples and the average values were taken for data analysis. The % equilibrium water uptake was calculated as

$$\left(\frac{\text{Mass of swollen beads } (w_1) - \text{Mass of dry beads } (w_2)}{\text{Mass of dry beads } (w_2)}\right) \times 100. \quad (1)$$

The standard deviation in water uptake was within 3.0%.

2.2.4. Drying rate of the beads

Immediately after the preparation of beads, a set of beads (≅0.5 g) that are representative of the batch varying in sizes from 925 to 1183 μm were kept in an incubator (Stuart Orbital Incubator, Model S150, Staffordshire, UK) maintained at 37 °C. The beads were weighed on an electronic microbalance (Mettler, AE 240, Switzerland) to an accuracy of ±0.01 mg at different time intervals. Initially, the beads were weighed at short intervals of time and later, at longer time intervals. Data were collected until attainment of constant mass, indicating the complete drying of the beads. Experiments were carried out in triplicate and the average values were used for calculations and plotting of data.

2.2.5. Drug content and entrapment efficiency

Estimation of drug content was done according to the method adopted earlier [30]. Beads of known weights were soaked in 50 mL water for 30 min and sonicated using a probe sonicator (UP 400 s, Dr. Hielscher GmbH, Germany) for 15 min to break the beads. The whole solution was centrifuged using a tabletop centrifuge (Jouan, MR 23i, France) to remove the polymeric debris. Then the polymeric debris was washed twice with fresh solvent (water) to extract any adhered drug. The clear supernatant solution was then analyzed for cephalexin content by a UV spectrophotometer (Secomam, Anthelie, France) at the λ_{max} value of 262 nm. The complete extraction of drug was confirmed by repeating the extraction process on the already extracted polymeric debris. The % entrapment efficiency of the matrix was then calculated as

Table 1
Formulation codes

% Drug loading	pH of the counterion media		
	5.0	7.0	9.0
25	F1	F5	F9
50	F2	F6	F10
75	F3	F7	F11
100	F4	F8	F12
25	C1[a]	C2[a]	C3[a]

[a] Control formulations prepared with only calcium as a counterion.

$$\%\ \text{Entrapment efficiency} = \frac{\text{Drug loading}}{\text{Theoretical drug loading}} \times 100. \quad (2)$$

These data for various formulations are presented in Table 2.

2.2.6. In vitro release studies

In vitro drug release from the different formulations of GG beads was investigated in 0.1 N HCl or pH 7.4 phosphate buffer media. These experiments were performed using the fully automated dissolution tester coupled with UV system (Logan Instruments Corp., Model D 800, NJ, USA) equipped with six baskets at the stirring speed of 100 rpm. A weighed quantity of each sample equivalent to 250 mg cephalexin was placed in 500 mL (aqueous solubility of cephalexin is 1 in 100 parts) of 0.1 N HCl or pH 7.4 phosphate buffer maintained at 37 °C. The instrument automatically measures the concentration of the drug released at the particular time intervals by UV spectrophotometer coupled with flowthrough cells attached with the instrument and then replaces the solution back into the dissolution bowl. The cephalexin concentration was determined spectrophotometrically at the λ_{max} value of 262 nm. These studies were performed in triplicate for each sample and the average values were used during data analysis.

2.2.7. Fourier transform infrared spectral studies

Fourier transform infrared (FTIR) spectra were taken on a Nicolet (Model Impact 410, Milwaukee, USA) instrument to investigate any possible chemical reactions between the drug and the polymer. FTIR spectra of the pure drug, placebo beads, and drug-loaded beads were obtained. All the samples were crushed with KBr to get the pellets by applying a pressure of 600 kg/cm^2. Spectral scanning was done in the range between 4000 and 500 cm^{-1}.

2.2.8. Differential scanning calorimetric analysis

Differential scanning calorimetry (DSC) was performed on pure cephalexin, placebo beads, and drug-loaded beads. DSC measurements were done on a Rheometric Scientific (DSC-SP, Surrey, UK) and about 8–10 mg of sample was heated from 25 to 300 °C at the heating rate of 10 °C/min in nitrogen atmosphere at the flow rate of 20 mL/min.

2.2.9. Scanning electron microscopic studies

Surface scanning electron microscopic (SEM) images were taken on the GG beads prepared in different pH media. Beads were sputtered with gold to make them conducting and placed on a copper stub. Scanning was done using Leica 400, Cambridge, UK instrument. Thickness of the gold layer obtained with gold sputtering was about 10 nm.

Statistical analyses were accomplished using SPSS statistical package. Analysis of variance followed by least significant difference procedure was used for the comparison of particle size and % entrapment efficiency of the beads.

3. Results and discussion

3.1. Preparation and characterization of beads

GG is an anionic deacetylated exocellular polysaccharide. Aqueous solution of GG is known to form hydrogels upon warming to body temperature (37 °C) as well as in the presence of cations [31]. Mechanism of hydrogel formation involves the formation of double helical junction zones followed by the aggregation of double helical segments to form a three-dimensional network by complexation with cations and hydrogen-bond formation with water [18].

Table 2
Results of % entrapment efficiency, bead size, parameters k and n, correlation coefficient (r) calculated from Eq. (16), and diffusion coefficients (D) calculated from Eq. (9) for sorption and desorption processes in pH 7.4 phosphate buffer

Formulation codes	% Entrapment efficiency	Volume mean bead size (μm)	k	n	r	$D_{(sorption)} \times 10^5$ (cm^2/s)	$D_{(desorption)} \times 10^8$ (cm^2/s)
F1	47.58	925	0.105	0.69	0.964	5.80	7.64
F2	54.50	958	0.109	0.66	0.958	5.82	7.71
F3	55.92	943	0.115	0.65	0.974	5.93	7.62
F4	59.22	934	0.118	0.62	0.982	6.01	7.70
F5	50.31	1029	0.086	0.72	0.966	2.18	7.15
F6	58.50	1060	0.090	0.71	0.988	2.38	7.24
F7	60.21	1048	0.093	0.70	0.972	2.49	7.18
F8	64.21	1039	0.099	0.70	0.985	2.72	7.23
F9	55.38	1183	0.075	0.76	0.969	0.629	6.83
F10	61.65	1122	0.078	0.74	0.971	0.631	6.77
F11	65.24	1136	0.081	0.73	0.986	0.653	6.72
F12	69.24	1151	0.086	0.72	0.978	0.688	6.91
C1	44.28	914	[a]	[a]	[a]	[a]	[a]
C2	49.13	1050	[a]	[a]	[a]	[a]	[a]
C3	53.36	1171	[a]	[a]	[a]	[a]	[a]

[a] Experiments not performed.

The strategy for ensuring hydrogelation in the present work is similar to that used earlier for the preparation of beads as well as microspheres from the ionic polymers such as alginate, chitosan, etc. [22]. The GG contains carboxylate side groups in glucuronosyl residues and hence, it can be crosslinked by inducing the ionic gelation with cations. Chan and Heng [27] reported that calcium and zinc cations exert varying effects on the morphology and drug release profiles of the alginate microspheres wherein, it was suggested that a combination of calcium and zinc cations could be employed to produce the microspheres with more sustained release characteristics. Kedzierewicz et al. [26] studied the CR of a highly water-soluble propranolol hydrochloride from the GG beads prepared by using calcium as a counterion. However, the release was too rapid for practical applications. These observations prompted us to use a combination of calcium and zinc as counterions for the hydrogelation of GG and thereby, for the easy encapsulation of cephalexin.

The % entrapment efficiency (see Table 2) of the GG beads for cephalexin varied between 47 and 69, depending upon the pH of the counterion media used for encapsulation. The % entrapment efficiency was the lowest for beads prepared in pH 5 media, whereas the highest % entrapment efficiency was observed for the beads produced in pH 9 media. This difference in the % entrapment efficiency may be attributed to the degree of ionization of carboxyl groups of GG in different pH media [31,32]. For instance, if there are less number of carboxylate groups on GG at pH 5, then calcium and zinc ions are less likely to crosslink and form a dense matrix that can entrap cephalexin successfully. The GG beads were spherical as revealed by the SEM images shown in Fig. 1. The pH of the counterion media appears to have a significant effect on the morphology and size of the beads. For instance, the beads prepared in pH 9 have smooth surfaces, while those prepared in pH 5 have a porous structure. This could be due to a more rapid approach of calcium and zinc ions to the surface of the GG droplet that has a higher anionic character at higher pH and thus, it forms a dense matrix. The size and size distribution of the beads were assessed by laser light diffraction technique (Mastersizer-2000, Malvern, UK). On a population basis, particle size distribution was found to be unimodal with narrow size distributions that are displayed for formulations F1, F5, and F9 in Fig. 2. Calculated values of volume-mean diameter of the beads are included in Table 2. These data showed that with increasing pH of the counterion media, bead size also increased. The higher bead size at higher pH may be the result of rapid migration of calcium and zinc ions to the surface of the GG droplet that has higher anionic character at higher pH. This has resulted in the immediate crosslinking of the droplets, which might have prevented the erosion of GG from the droplets.

It would be instructive to suggest a correlation between % entrapment efficiency with the size of the beads (see Table 2). For instance, with increasing the pH of the counterion media from 5 to 9 (formulations F1, F5, and F9), the

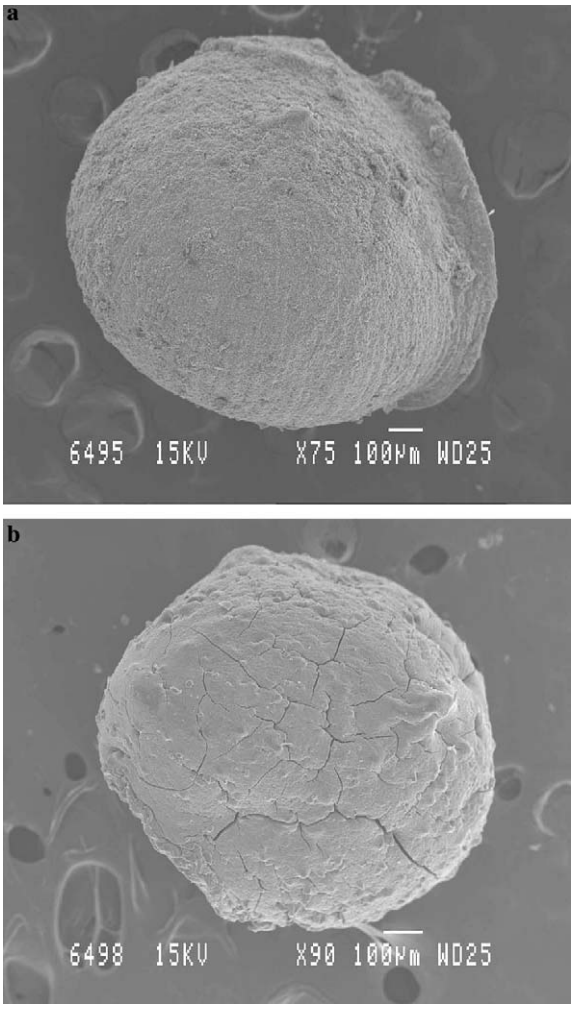

Fig. 1. SEM images of beads produced in: pH 9 (a) and pH 5 (b) media.

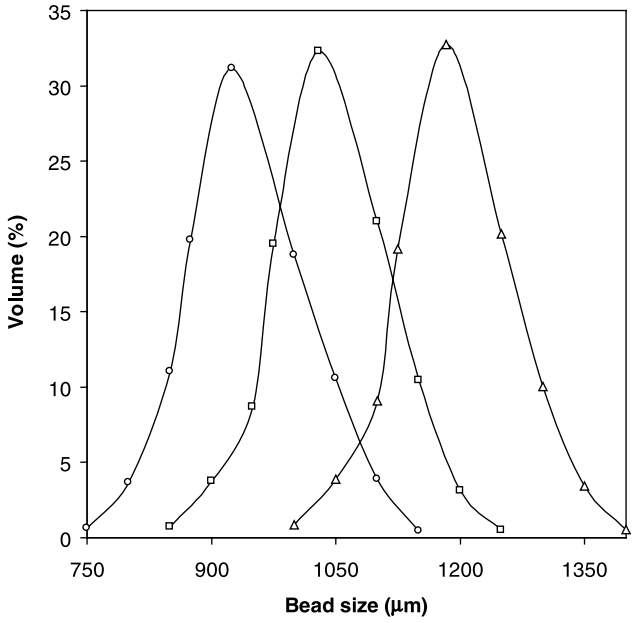

Fig. 2. Particle size distribution of beads with 25% drug loading prepared in: pH 5 (○), pH 7 (□), and pH 9 (△) media.

% entrapment efficiency also increased considerably from 47.6 to 55.4, while the mean volume diameter increased systematically from 925 to 1183 μm. On the other hand, for formulations F2, F6, and F10, % entrapment efficiency increased systematically from 54.5 to 61.7, while the volume mean bead size increased from 958 to 1122 μm. For formulations F3, F7, and F11, the % entrapment efficiency increased from 55.9 to 65.2, while the bead size showed a systematic variation from 943 to 1136 μm. Similarly, for formulations F4, F8, and F12, both % entrapment efficiency and particle size increased systematically from 59.2 to 69.2 and 934 to 1151 μm, respectively. The size and % entrapment efficiency of the beads prepared in counterion media with pH 5, 7 or 9 are further statistically evaluated by analysis of variance (ANOVA). The F value for bead size was found to be 111.7 (degree of freedom (df) = 35, $P < 0.01$), indicating a highly significant difference in the sizes of the beads prepared in three different pH media. The ANOVA was further extended by the least significant difference (LSD) procedure. The results indicate that beads prepared in pH 5 media are significantly different in size from those prepared in pH 7 media and also, beads prepared in pH 7 media are significantly different in size from those prepared in pH 9 media. Similarly, F value for % entrapment efficiency was found to be 7.298 (df = 35, $P < 0.05$), which indicates that there is a significant difference in the % entrapment efficiency of beads prepared in three different pH media. Similarly, here also ANOVA was extended by the least significant difference (LSD) procedure. The results indicate that % entrapment efficiency of the beads prepared in pH 5 media is significantly different from those prepared in pH 9 media. Similarly, % entrapment efficiency of beads prepared in pH 7 media is significantly different from those prepared in pH 9 media; however, there is no significant difference in % entrapment efficiency between the beads prepared in pH 5 and pH 7 media. A similar trend is followed in case of control formulations C1, C2, and C3, the % entrapment efficiency and bead sizes increasing systematically from 44.3 to 53.4 and 914 to 1171 μm, respectively, with an increasing pH of counterion media from 5 to 9.

In an effort to investigate the possible chemical interactions of the drug with the hydrogel matrix, we have analyzed: (a) pure cephalexin, (b) placebo beads, and (c) cephalexin-loaded beads using FTIR. These spectra are displayed in Fig. 3. In case of placebo beads, a broad peak appeared at 3419 cm^{-1} due to the presence of hydroxyl groups of glucopyranose ring that are hydrogen-bonded to various degrees. The bands appearing at 1622 and 1412 cm^{-1} are due to asymmetric and symmetric stretchings of carboxylate group. The band at 2925 cm^{-1} is due to stretching vibration of $-CH_2$ group, while those appearing at 1159 and 1029 cm^{-1} are due to ethereal and hydroxylic C–O stretchings. Bending vibration of C–H appeared at 887 cm^{-1}. Cephalexin has shown a characteristic band at 3438 cm^{-1} due to the amide N–H stretching vibrations. The bands at 3271 and 3209 cm^{-1} are due to intermolecular hydrogen-bonded amine groups while a band at 3042 cm^{-1} is due to the acidic hydroxyl groups. Characteristic bands appearing at 1758 and 1690 cm^{-1} are due to four-membered lactam carbonyl and secondary amide carbonyl groups, respectively. The bands at 1591 and 2919 cm^{-1} are due to N–H bending vibrations and C–H stretching vibrations, respectively. The bands appearing at 1455, 1406, and 1350 cm^{-1} are due to C–H bending vibrations. The C–N stretching vibrations are observed at 1283 cm^{-1}, whereas C–O stretching vibrations are observed at 1073 cm^{-1}. Characteristic peaks due to monosubstituted phenyl groups appeared at 745 and 696 cm^{-1}, whereas the peak due to C–S stretching vibrations has merged at 745 cm^{-1}. Spectra of the drug-loaded GG beads are not characteristically different from the spectra of pristine GG beads. Peaks appearing at 1752, 1412, 1283, 1079, and 702 cm^{-1} for cephalexin have also appeared in the drug-loaded beads, indicating the chemical stability of cephalexin after entrapment. However, bands appearing at 1690 cm^{-1} in cephalexin and 1622 cm^{-1} in GG have appeared in drug-loaded beads at 1635 cm^{-1}, indicating the weak interaction of quaternary ammonium salt type between primary amine group of the drug with that of carboxylate group of GG. However, this kind of interaction disappears to release the primary amine group of drug effectively in the basic pH conditions of the intestine.

DSC thermograms for pure cephalexin (a), placebo beads (b), and cephalexin-loaded beads (c) are presented in Fig. 4. The crystallinity of cephalexin and melting temperature (T_m) of the polymer were determined. Placebo beads have shown an endothermic peak at 252 °C, indicating the melting temperature of the polymer, whereas cephalexin-loaded beads showed an endothermic peak at 248 °C. This slight decrease in the melting temperature may be due to minor physical and morphological changes taking place in the beads after the drug loading. For pure cephalexin, an endothermic peak appeared at 194 °C due to the melting of the drug, but this peak has not appeared in all the cephalexin-loaded beads, indicating an amorphous dispersion of the drug into the polymer matrix.

3.2. Dynamic swelling studies

Swelling studies of the formulations are important to assess the hydrogelation of the beads formed. Dynamic swelling experiments were carried out gravimetrically in 0.1 N HCl or pH 7.4 phosphate buffer. Since no significant difference ($P < 0.01$) was observed in the sorption of beads between both the media studied, hence only the % weight gain raw data obtained in pH 7.4 phosphate buffer are displayed in Fig. 5 for some representative formulations F1, F5, and F9. It is observed that higher weight gain of the beads in pH 5 media was more prominent just before attainment of equilibrium swelling or more appropriately sorption. However, the beads prepared in pH 9 media showed a more rigid structure and hence, lesser swelling than those prepared in pH 5 or 7 media. The beads (F9)

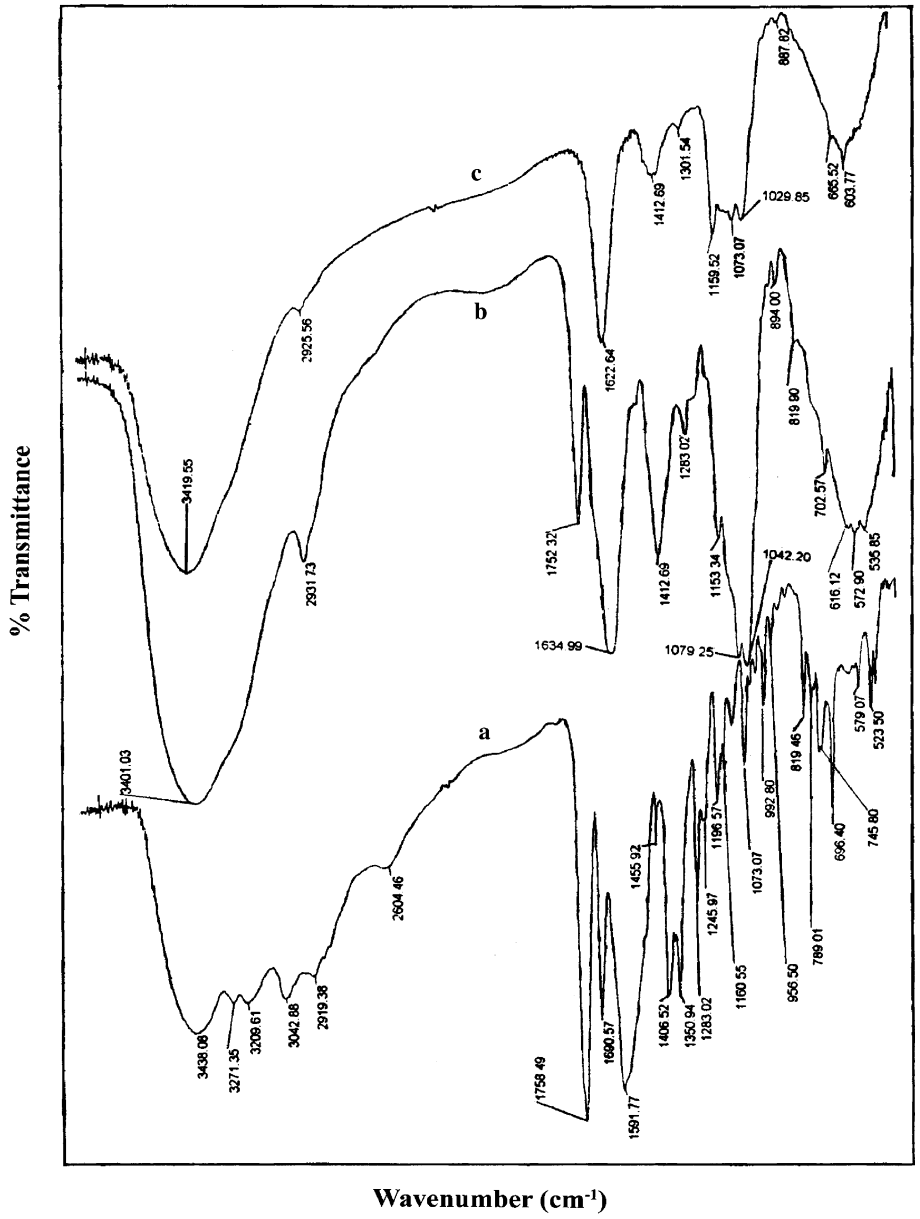

Fig. 3. FTIR spectra of: pure cephalexin (a), cephalexin-loaded beads (b), and placebo beads (c).

prepared in pH 9 media attained equilibrium sorption quite fast (ca. 100 min), but experiments were continued until longer time (ca. 300 min) to ensure complete equilibration. Beads produced in pH 5 media have shown the maximum swelling up to 175% of the dry mass of the polymer.

3.3. Drying rate of the beads

In order to optimize the drying conditions and to evaluate the effect of processing variables on the drying of beads, few beads representative of the batch were selected. The raw data of weight loss (mg) as a function of time are displayed in Fig. 6 for the formulations that were chosen for swelling studies, i.e., F1, F5, and F9. The results indicate that beads produced in pH 5 media dried quicker than those produced in pH 9 media. This could be attributed to the porous nature of the beads produced in pH 5, thereby allowing higher evaporation loss of liquids from the beads. Also, it could be attributed to the rigidity of the hydrogel matrix formed at higher pH.

3.4. Diffusion coefficients for liquid transport through spherical beads

In the present study, cephalexin is dispersed in almost spherically shaped beads. It would be of interest to model the transport process to compute the diffusion coefficient, D and to study its effect in terms of concentration profiles generated within the beads. Diffusion occurs due to the immersion of the beads into the medium of interest. Mathematical models are available [29,33] to describe the sorption and desorption processes under the simulated test

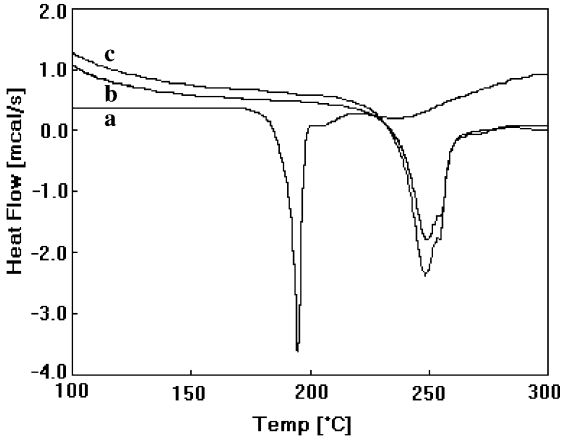

Fig. 4. DSC thermograms of: pure cephalexin (a), placebo beads (b), and cephalexin-loaded beads (c).

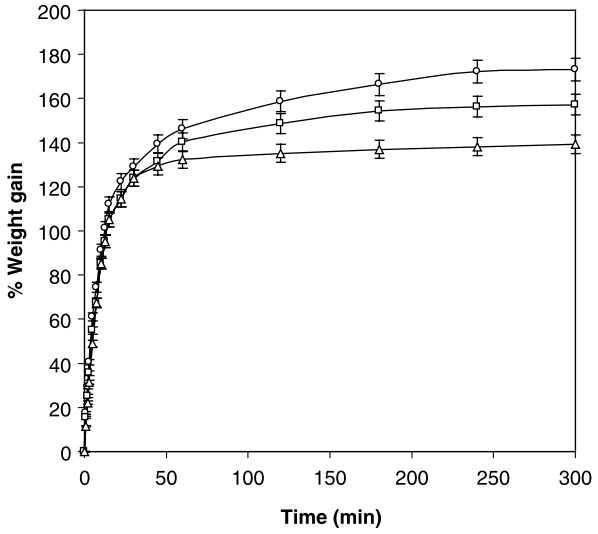

Fig. 5. Effect of pH of counterion media on % water uptake by the beads with 25% drug loading prepared in: pH 5 (○), pH 7 (□), and pH 9 (△) media.

conditions. For a spherical geometry, the change in concentration inside the spherical bead of radius, r can be described by Fick's equation [33].

$$F = -D\left[\frac{\partial C}{\partial r}\right]. \tag{3}$$

Here, F is flux (matter transported per unit area and unit time) and $\partial C/\partial r$ represents the concentration gradient. The following assumptions were considered for predicting concentration profiles of liquids within the spherical beads.

1. Dosage form is spherical and drug is uniformly dispersed in it (as proved by DSC).
2. Radial transports are considered wherein both the matter transport takes place simultaneously, i.e., (i) the liquid enters the polymer and (ii) the drug leaves the dosage form. Both these transports are controlled by the transient diffusion and are related to each other.

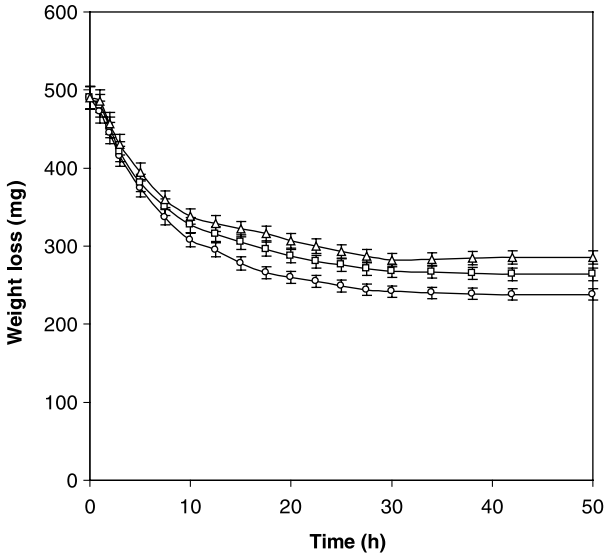

Fig. 6. Effect of pH of counterion media on the drying rate of the beads with 25% drug loading prepared in: pH 5 (○), pH 7 (□), and pH 9 (△) media.

3. Diffusion coefficients of both the transports depend on concentrations of the drug and the liquid.
4. Despite matrix swelling, a frame of reference is fixed with respect to the initial dosage form for all calculations.

Fick's equation for radial diffusion with a concentration-dependent diffusivity is given as

$$\frac{\partial C}{\partial t} = \frac{1}{r^2}\cdot\frac{\partial}{\partial r}\left[D\cdot r^2\cdot\frac{\partial C}{\partial r}\right]. \tag{4}$$

Diffusion in spherical beads can be described by using the Laplace transformation of Fick's equation to calculate the mass uptake (or more appropriately release in the present context), by the beads using,

$$\frac{M_t}{M_\infty} = 6\sqrt{\frac{Dt}{\pi^2}}\left(\frac{1}{\sqrt{\pi}} + 2\sum_{n=1}^{\infty}\mathrm{ierf}\ \frac{nr}{\sqrt{Dt}}\right) - 3\frac{Dt}{r^2}, \tag{5}$$

where M_t is the amount of liquid released at time, t and M_∞ is the total amount of liquid in the spherical bead. Eq. (5) is quite complicated to solve, but Baker and Lonsdale [34] have derived the following equation that is appropriate for the present case under the initial and boundary conditions, set as follows:

Initial: $t = 0 \quad r < R \quad C = C_{\mathrm{in}}$ (inner part of beads)

Boundary: $t > 0 \quad r = R \quad C = C_{\mathrm{eq}}$ (surface of beads)

In the above equations, R is radius of the sphere and r is radius of the small concentric shell within the spherical bead. It may be noted that the analytical solution for the above problem does not exist, essentially because of the double transport (i.e., simultaneous transport of liquid and drug) as well as the much-complicated problem of concentration dependence of D.

$$\frac{M_t}{M_\infty} = 6\sqrt{\frac{Dt}{\pi R^2}} - \frac{3Dt}{R^2}. \quad (6)$$

Eq. (6) is thus valid for $M_t/M_\infty < 0.4$, but at longer times, i.e., for sorption $M_t/M_\infty > 0.6$, the liquid release profile is given by

$$\frac{M_t}{M_\infty} = 1 - \frac{6}{\pi^2}\exp\left(-\frac{\pi^2 Dt}{R^2}\right). \quad (7)$$

At intermediate time intervals: $0.4 \leqslant M_t/M_\infty \leqslant 0.6$, both Eqs. (6) and (7) do not give a good approximation within ±5% of the theoretical profile given by Eq. (5). Thus, for a constant diffusivity, i.e., at short-term sorption, when the amount of liquid or drug transported is low (i.e., $M_t/M_\infty < 0.4$), M_t is proportional to square root of time, $t^{1/2}$ and hence,

$$\frac{M_t}{M_\infty} = \frac{6}{R}\left[\frac{Dt}{\pi}\right]^{1/2}. \quad (8)$$

The above equation is valid for the initial drug release (i.e., $M_t/M_\infty \leqslant 0.4$) and it gives the well-known $t^{1/2}$ dependence of the release profile. Diffusion coefficient can then be calculated for water absorption or drug release by the beads using,

$$D = \left(\frac{R\theta}{6M_\infty}\right)^2 \pi. \quad (9)$$

Here, θ is slope of the linear portion of the plot of M_t/M_∞ vs. $t^{1/2}$ when there is no lag-time for diffusion, R is radius of the beads, and M_∞ is the maximum sorption value. The value of θ was computed from the least-squares procedure at 95% confidence level. Only those values giving the correlation coefficient of $r > 0.99$ were selected. The plots of M_t/M_∞ vs. $t^{1/2}$ for liquid sorption from the beads during sorption process are displayed in Fig. 7. It is observed that the initial portions of the sorption curves in all the formulations exhibited slight sigmoidal trends, suggesting the deviation in transport phenomenon from the ideal Fickian behavior to anomalous case, i.e., strange case. However, the equilibrium sorption occurred for all the formulations at around $t^{1/2} = 15\ \mathrm{h}^{1/2}$.

Drying results of the beads presented in Fig. 6 were converted into desorption rate, i.e., $(1 - M_t/M_\infty)$ and these data are now displayed in Fig. 8 for the same formulations as presented in Fig. 7. We observed a slight lag-time initially, but later, the desorption curves increased considerably up to 10 h and then leveled around 20 h for all the formulations. Since the curves are overcrowded within a short interval values of $\ln(1 - M_t/M_\infty)$ and hence, it was difficult to comment on these data for the individual formulations. Values of D were calculated by following the same procedure as before for sorption data, i.e., from the initial slopes of the linear portion of $\ln(1 - M_t/M_\infty)$ vs. t as shown in Fig. 8.

Values of D calculated for sorption and desorption processes are included in Table 2. It is observed that the values of D for sorption are higher than those observed for

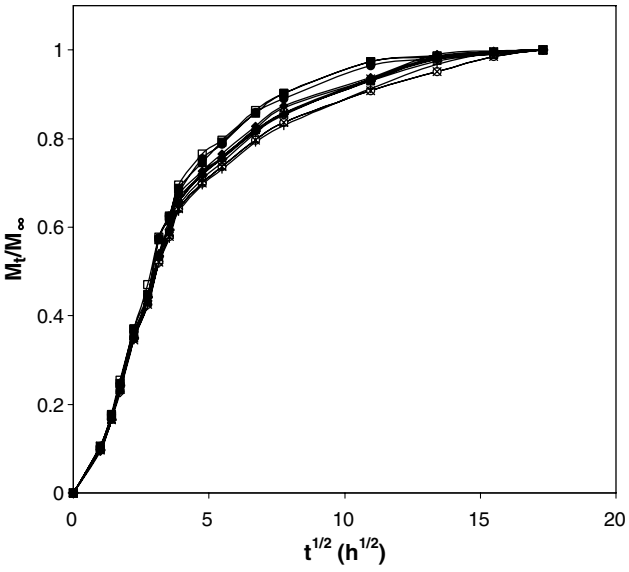

Fig. 7. Plot of M_t/M_∞ as a function of square root of time for liquid sorption from beads with: 25% drug loading prepared in pH 5 (○), pH 7 (◇), and pH 9 (+) media; 50% drug loading prepared in pH 5 (●), pH 7 (◆), and pH 9 (×) media; 75% drug loading prepared in pH 5 (□), pH 7 (△), and pH 9 (∗) media and 100% drug loading prepared in pH 5 (■), pH 7 (▲), and pH 9 (—) media.

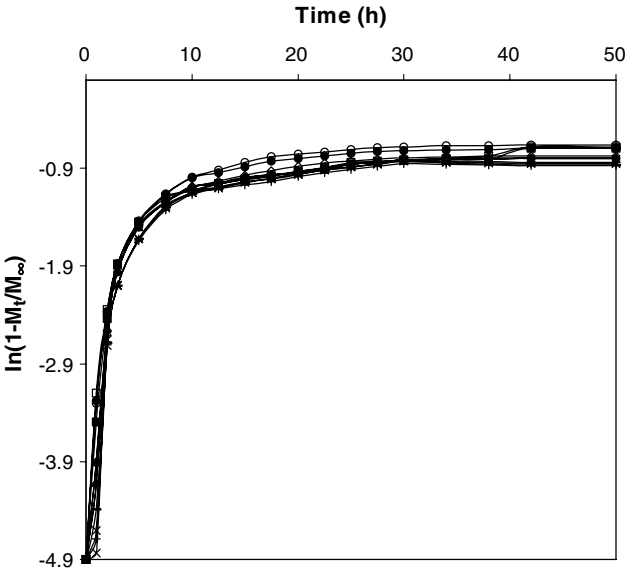

Fig. 8. Plot of $\ln(1 - M_t/M_\infty)$ as a function of time for liquid desorption from beads with: 25% drug loading prepared in pH 5 (○), pH 7 (◇), and pH 9 (+) media; 50% drug loading prepared in pH 5 (●), pH 7 (◆), and pH 9 (×) media; 75% drug loading prepared in pH 5 (□), pH 7 (△), and pH 9 (∗) media and 100% drug loading prepared in pH 5 (■), pH 7 (▲), and pH 9 (—) media.

desorption by nearly three orders of magnitude. This trend is in good agreement with the earlier literature [9]. This is due to slower drying of the beads compared to the rapid liquid sorption of the aqueous media by the beads. Sorption of liquid occurs due to diffusion, whereas desorption is a diffusion-controlled evaporation of the liquid. However, the process of evaporation is controlled by diffusion in

the sense that the rate of evaporation depends largely on the rate at which solvent is supplied to the evaporating surface as a result of diffusion of liquid. During sorption, when the sample is in contact with the liquid, the concentration of liquid on the surface reaches equilibrium as soon as sorption starts. However, in case of desorption, the rate of evaporation is proportional to the difference in liquid concentration on the surface to the space at the center of the bead [29]. Diffusion coefficients for sorption decreased systematically with increasing pH value from 5 to 9 of the counterion media. The D values for sorption of the beads prepared in pH 5 media varied from 5.80×10^{-5} to 6.01×10^{-5} cm^2/s, whereas for beads prepared in pH 9 media, these ranged between 6.29×10^{-6} and 6.88×10^{-6} cm^2/s. Such lower D values confirmed the more rigid nature of the beads formed in pH 9 media. However, for beads prepared in pH 5 media, the network structure is somewhat loose, which would create a high hydrodynamic free volume in the matrix to accommodate more solvent molecules, thus inducing the matrix swelling. Lower water uptake and diffusion values observed in beads prepared in pH 9 media further confirmed the formation of a rigid matrix. The increase in D values with increasing drug loading may be due to a slight decrease in the rigidity of the polymer matrix in the presence of dispersion of the drug.

3.5. Numerical analysis of the transport phenomenon – calculation of concentration profiles

The complex problem of double transport in bead geometry discussed earlier was further investigated by using an explicit numerical method with the finite difference approach method as was originally suggested by Vergnaud [29]. Here, the polymeric bead was divided into concentric spheres of varying radii, $r + \Delta r$, r, and $r - \Delta r$. The number of concentric spheres is related to the radial thickness, Δr of each spherical part. Each position in the radial direction within the sphere is defined by an integer, n:

$$r = n \cdot \Delta r. \tag{10}$$

The concentrations of drug and liquid are constant within each spherical part of thickness, Δr located between two adjacent spheres, at the same time, t. The matter balance can then be calculated for the short lapse of time, Δt within the spherical part of thickness, Δr and centered on the position, r defined by the integer, n using Fick's first law as per the matrix space-time diagram shown in Fig. 9.

New concentration (CN_n) within the bead at position, r (integer, n) after lapse of time, Δt is expressed in terms of concentration at the previous times (C_n) in the same place and in the two adjacent planes.

$$CN_n = C_n + \frac{\Delta t}{n^2(\Delta r)^2} \cdot \left[J_{n-1/2} - J_{n+1/2}\right]. \tag{11}$$

Here, J is a function of diffusivity and concentration, which may be written as

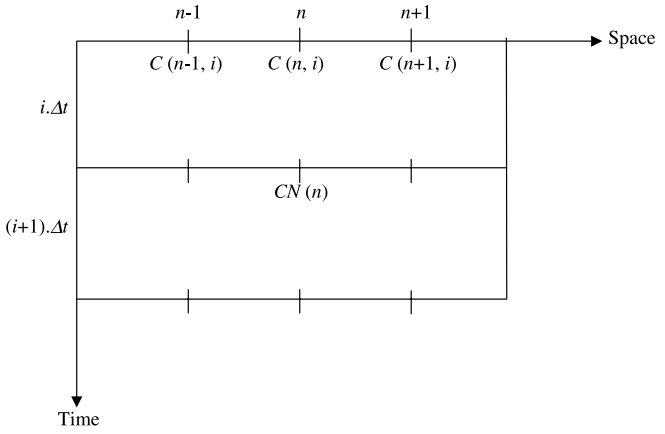

Fig. 9. Scheme used for spherical geometry in numerical analysis.

$$J_{n-1/2} = (n - 1/2)^2 \cdot D_{n-1/2} \cdot (C_{n-1} - C_n). \tag{12}$$

Thus, diffusivity at the intermediate position $(n - 1/2)$ can be computed from the diffusivities at positions, n and $n + 1$, by either way. In the program, we have assumed the zero concentration (C_0) at the center of the sphere and then calculated the matter balance for the sphere of radius, $\Delta r/2$ located in the middle of the bead. The concentration of the drug and the liquid on the surface of the beads represents the concentration at equilibrium (C_{eq}) following the second assumption. Thus, the concentration, C_0 at the center of the sphere is considered to equal to that in the bead (as a whole) at time zero, i.e.,

$$C_0 = C_{eq} \text{ liquid, drug.} \tag{13}$$

The amount of drug remaining (or liquid entered) in the beads at time, t was then obtained by integrating the concentration of the drug at this time with respect to space

$$M_t = 4\pi \cdot \int_0^R r^2 \cdot C_{r \cdot t} \cdot \mathrm{d}r. \tag{14}$$

This expression was rewritten using the finite differences as

$$M_t = 4\pi(\Delta r)^3 \cdot \left[\frac{C_0}{24} + \sum_{n=1}^{n-2} n^2 C_n + \frac{9}{8}(n-1)^2 C_{n-1} + \frac{3}{8} n^2 \cdot C_n\right]. \tag{15}$$

The preceding equations were used to compute the concentration at any place and at any time, either for liquid or drug, since their diffusivities are known. Then, one can obtain the plot of M_t (as calculated from Eq. (15)) vs. $t^{1/2}$ for 25%, 50%, 75%, and 100% drug loading or liquid entering as shown in Fig. 10. It was observed that the theoretical curves generated for the different drug loadings even though originate from zero, but they all exhibited some lag-time in the beginning. However, the M_t values calculated followed the trend that at higher loading of the drug, higher release was occurred.

Concentration profiles of the migrating liquid developed inside the dosage form during the diffusion process are displayed in Fig. 11. It is the attainment of equilibrium that

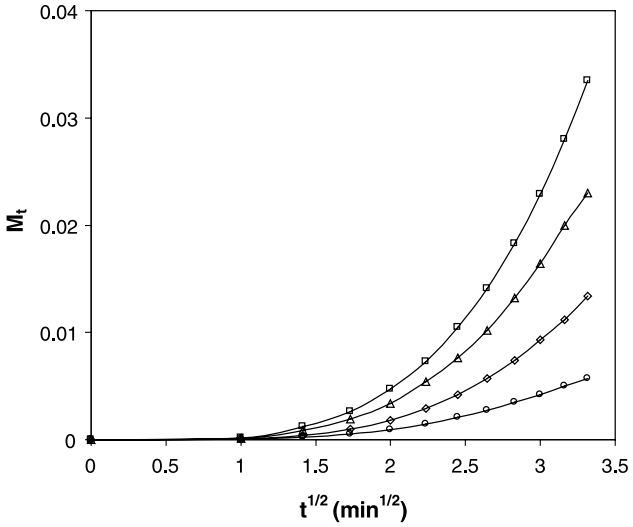

Fig. 10. Plot of M_t calculated from Eq. (15) as a function of $t^{1/2}$ for: 25 % (○), 50 % (◇), 75% (△), and 100% (□) drug loadings.

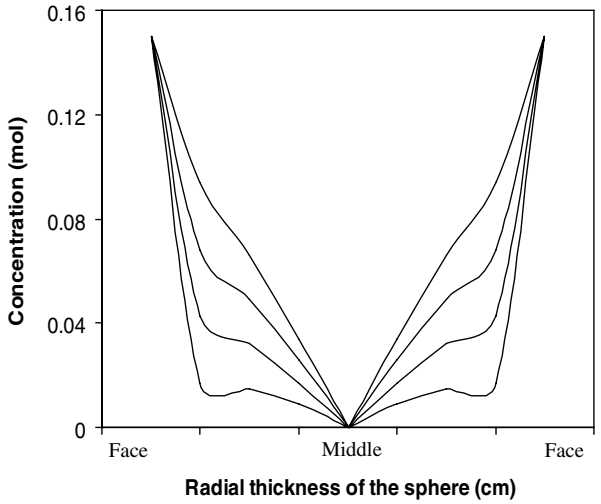

Fig. 11. Penetrant concentration profiles developed inside the drug-loaded beads.

will eventually exist between the concentration in the gel bead and the concentration in the bulk that encourages the remainder of the drug to remain in the bead. Thus, the steep gradients of concentration of liquid and drug were developed in the dosage form, especially next to the surface. This gave the concentration profile of the migrating liquid as minimum at the center of the sphere, but extended to large values near the surface. Each curve in Fig. 11 refers to the concentration of solvent at different time intervals at every 30 min interval. Since it is possible that transport can also take place in one dimension and the contribution of each spherical slice to the transport will not be the same, and therefore, the volume of each slice could be proportional to the radius squared. Under these conditions, the behavior of the external slice was more effective than that of the internal slice, which has a smaller radius. Therefore, the concentration at position $n - 1/2$ would give the mean value of those in adjacent places, i.e., n and $n + 1$.

3.6. In vitro drug release

In vitro drug release studies were performed in 0.1 N HCl or pH 7.4 phosphate buffer for 6 h. Since there was no significant difference ($P < 0.01$) of the drug release in both the media, only the data obtained in pH 7.4 phosphate buffer are presented in Fig. 12 for different loadings of cephalexin in the beads. The effect of drug loading on the release rates was investigated for formulations F9, F10, F11, and F12. The release rates were slower for formulations containing lower amount of the drug, while the release rate increased with increasing amount of drug in the beads. The release rate can be correlated with the diffusion coefficient (see Table 2), which indicates that as the diffusion coefficient increases (for formulations F9, F10, F11, and F12), the release rate also has increased. The drug in the beads might act as inert filler by occupying the free volume of the swollen hydrogel. This could have created a tortuous path for water molecules to permeate, but the degree of tortuosity depends upon the volume fraction of the filler [35]. However, for all formulations, the release rate was extended up to 6 h. The results of % cumulative release vs. time for beads prepared in counterion media having three different pH values, loaded with 25% of cephalexin, are presented in Fig. 13. Drug release rates were higher for beads prepared in the counterion media having pH 5 compared to those prepared in pH 9 media. This could be attributed to the formation of a rigid matrix in higher pH media. At lower pH, possibly less number of carboxylates are available for matrix crosslinking than at higher pH. The SEM images indicated that beads prepared

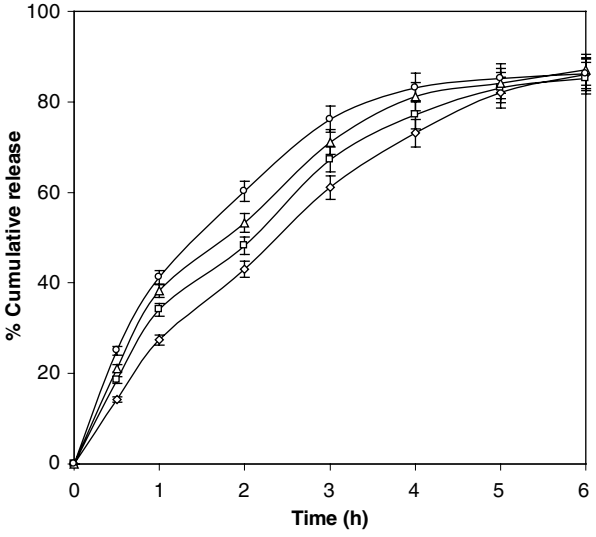

Fig. 12. Effect of % drug loading on in vitro release profiles for beads prepared in pH 9 media with: 25% (◇), 50% (□), 75% (△), and 100% (○) drug loadings.

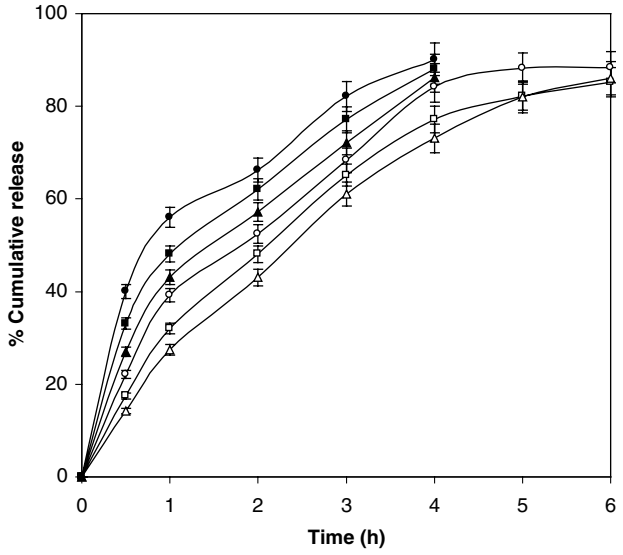

Fig. 13. Effect of pH of counterion media on in vitro release profiles for formulations with 25% drug loading prepared in: pH 5 (○), pH 7 (□), and pH 9 (△) media and for control formulations with 25% drug loading prepared in pH 5 (●), pH 7 (■), and pH 9 (▲) media.

in the counterion media having pH 5 have a porous structure, while those prepared in pH 9 media have the smooth surfaces. This could be another reason for the fast drug release rates, since the porous matrices allowed faster diffusion of the drug into the dissolution media than the rigid beads. Similarly, here also a correlation between diffusion coefficient and release rate can be established. It can be observed that for formulations F1, F5, and F9, the diffusion coefficient decreased from 5.8×10^{-5} to $0.629 \times 10^{-5}\,\mathrm{cm^2/s}$ and the release rates also showed a drastic decrease (see Fig. 13). The results of control formulations (C1, C2, and C3) are also compared in Fig. 13.

The initial 60% drug release data were analyzed using the empirical equation proposed by Ritger and Peppas [28] by fitting to Eq. (16).

$$\frac{M_t}{M_\infty} = kt^n. \tag{16}$$

A least-squares method at 95% confidence level was used to estimate the values of the parameter, k and diffusional exponent, n. These data along with the values of the correlation coefficient, r are included in Table 2. The values of k increase with increasing % loading of cephalexin in the beads, but the values of n decrease with increasing % loading of cephalexin. This indicates the smaller level interactions between the beads and the swelling media with increasing size of the beads. The values of n are in the range of 0.62–0.76. These indicated that the drug release was deviated only slightly from the Fickian trend and followed the anomalous trend.

4. Conclusions

Gellan gum beads of narrow size distribution with volume mean diameter ranging between 925 and 1183 μm were prepared by the cation-induced ionotropic gelation method. Beads prepared in acidic pH media showed a porous structure, while those prepared in basic media have the smooth surfaces. Different % entrapment efficiency of cephalexin was observed by varying the % drug loading as well as the pH of the counterion media. Release rates were higher when the % loading of cephalexin was higher. Similarly, the beads prepared in acidic pH media gave higher release rates. However, no significant difference in the release rates could be seen in 0.1 N HCl or pH 7.4 phosphate buffer media. The n values indicated the release mechanism to be slightly deviated from the ideal Fickian trend. This work demonstrates that by using a combination of calcium and zinc as the counterions, one could produce the more sustained release formulations using gellan gum beads compared to the use of calcium ions alone. Thus, it is necessary to use the combination of calcium and zinc cations to produce the uniform size gellan gum beads having sustained drug release properties. The simulation procedure successfully computed the concentration profiles of drug transport through the beads as well as it helped in explaining the double transport processes taking place while studying the drug release characteristics of the beads.

Acknowledgments

Authors appreciate the financial support from the University Grants Commission (UGC), New Delhi, India (F1-41/2001/CPP-II) to establish the Center of Excellence in Polymer Science.

References

[1] N.A. Peppas, Hydrogels in Medicine, CRS Press, Boca Raton, FL, 1986.
[2] F. Alhaique, E. Santucci, M. Carafa, T. Coviello, E. Murtas, F.M. Riccieri, Gellan in sustained release formulations: preparation of gel capsules and release studies, Biomaterials 17 (1996) 1981–1986.
[3] M.V. Risbud, R.R. Bhonde, Polyacrylamide-chitosan hydrogels: in vitro biocompatibility and sustained antibiotic release studies, Drug Deliv. 7 (2000) 69–75.
[4] K.S. Soppimath, T.M. Aminabhavi, A.M. Dave, S.G. Kumbar, W.E. Rudzinski, Stimulus-responsive smart hydrogels as novel drug delivery systems, Drug Dev. Ind. Pharm. 28 (2002) 957–974.
[5] V. Kudela, Hydrogels, in: H.F. Mark (Ed.), Encyclopedia of Polymer Science and Engineering, vol. 7, Wiley, New York, 1989, pp. 703–807.
[6] N.A. Peppas, P. Buresa, W. Leobandunga, H. Ichikawab, Hydrogels in pharmaceutical formulations, Eur. J. Pharm. Biopharm. 50 (2000) 27–46.
[7] A.S. Hoffman, Hydrogels for biomedical applications, Adv. Drug Del. Rev. 54 (2002) 3–32.
[8] A.R. Kulkarni, K.S. Soppimath, T.M. Aminabhavi, Controlled release of diclofenac sodium from sodium alginate beads crosslinked with glutaraldehyde, Pharma. Acta Helv. 74 (1999) 29–36.
[9] A.R. Kulkarni, K.S. Soppimath, T.M. Aminabhavi, A.M. Dave, M.H. Mehta, Glutaraldehyde crosslinked sodium alginate beads containing liquid pesticide for soil application, J. Control. Release 63 (2000) 97–105.
[10] A.R. Kulkarni, K.S. Soppimath, T.M. Aminabhavi, W.E. Rudzinski, In vitro release kinetics of cefadroxyl-loaded sodium alginate interpenetrating network beads, Eur. J. Pharm. Biopharm. 51 (2001) 127–133.

[11] K.S. Soppimath, A.R. Kulkarni, T.M. Aminabhavi, Chemically modified polyacrylamide-*g*-guar gum based cross-linked anionic microgels as pH-sensitive drug delivery systems: preparation and characterization, J. Control. Release 75 (2001) 331–345.
[12] M. Horii, T. Morinaga, S. Shimada, T. Takeuchi, H. Yamanaka, T. Nishimura, Y. Noshi, T. Okada, T. Sasaki, S. Ikeda, S. Takada, O. Iizuka, J. Kimura, S. Sagara, Y. Inada, Y. Nishioka, M. Kimata, Double-blind comparison of L-keflex and cephalexin (Keflex) in dental infections, Jpn. J. Antibiot. 33 (1980) 1194–1214.
[13] S.A. Agnihotri, T.M. Aminabhavi, Formulation and evaluation of novel tableted chitosan microparticles for the controlled release of clozapine, J. Microencapsul. 21 (2004) 709–718.
[14] K.S. Kang, G.T. Veeder, P.J. Mirrasoul, T. Kaneko, I.W. Cottrell, Agar-like polysaccharide produced by *Pseudomonas* species: production and basic properties, Appl. Environ. Microbiol. 43 (1982) 1086–1091.
[15] P.E. Jansson, B. Lindberg, P.A. Sandford, Structural studies of gellan gum an extracellular polysaccharide elaborated by *Pseudomonas elodea*, Carbohydr. Res. 124 (1983) 135–139.
[16] M.S. Kuo, A.J. Mort, A. Dell, Identification and location of L-glycerate an unusual acyl substituent in gellan gum, Carbohydr. Res. 156 (1986) 173–187.
[17] G.R. Sanderson, R.C. Clark, Gellan gum, Food Technol. 37 (1983) 62–70.
[18] H. Grasdalen, O. Smidsroed, Gelation of gellan gum, Carbohydr. Polym. 7 (1987) 371–393.
[19] Y.D. Sanzgiri, S. Maschi, V. Crescenzi, L. Callegaro, E.M. Topp, V.J. Stella, Gellan-based systems for ophthalmic sustained delivery of methylprednisolone, J. Control. Release 26 (1993) 195–201.
[20] A. Rozier, C. Mazuel, J. Grove, B. Plazonnet, Functionality testing of gellan gum, a polymeric excipient material for ophthalmic dosage forms, Int. J. Pharm. 153 (1997) 191–198.
[21] W. Kubo, S. Miyazaki, D. Attwood, Oral sustained delivery of paracetamol from in situ-gelling gellan and sodium alginate formulations, Int. J. Pharm. 258 (2003) 55–64.
[22] S. Miyazaki, N. Kawasaki, W. Kubo, K. Endo, D. Attwood, Comparison of in situ gelling formulations for the oral delivery of cemetidine, Int. J. Pharm. 220 (2001) 161–168.
[23] S. Miyazaki, H. Aoyama, N. Kawasaki, W. Kubo, D. Attwood, In situ-gelling gellan formulations as vehicles for oral drug delivery, J. Control. Release 60 (1999) 287–295.
[24] K.J. Quigley, P.B. Deasy, Use of deacetylated gellan gum (Gelrite) for the production of sulphamethizole containing beads, J. Microencapsul. 9 (1992) 1–7.
[25] E.A. el Fattah, D.J. Grant, K.E. Gabr, M.M. Meshali, Physical characteristics and release behavior of salbutamol sulfate beads prepared with different ionic polysaccharides, Drug Dev. Ind. Pharm. 24 (1998) 541–547.
[26] F. Kedzierewicz, C. Lombry, R. Rios, M. Hoffman, P. Maincent, Effect of the formulation on the in-vitro release of propranolol from gellan beads, Int. J. Pharm. 178 (1999) 129–136.
[27] L.W. Chan, Y. Jin, P.W.S. Heng, Cross-linking mechanisms of calcium and zinc in production of alginate microspheres, Int. J. Pharm. 242 (2002) 255–258.
[28] P.L. Ritger, N.A. Peppas, A simple equation for description of solute release. II. Fickian and anomalous release from swellable devices, J. Control. Release 5 (1987) 37–42.
[29] J.M. Vergnaud, Liquid Transport Processes in Polymeric Materials. Modeling and Industrial Applications, Prentice Hall, Englewood Cliffs, NJ, 1991.
[30] S.A. Agnihotri, T.M. Aminabhavi, Controlled release of clozapine through chitosan microparticles prepared by a novel method, J. Control. Release 96 (2004) 245–259.
[31] V. Crescenzi, M. Dentini, T. Coviello, Solution and gelling properties of microbial polysaccharides of industrial interest: the case of gellan, in: E.A. Dawes (Ed.), Novel Biodegradable Microbial Polymers, Kluwer Academic Publishers, The Netherlands, 1990, pp. 227–284.
[32] H. Moritaka, K. Nishinari, M. Taki, H. Fukuba, Effects of pH, potassium chloride, and sodium chloride on the thermal and rheological properties of gellan gum gels, J. Agric. Food Chem. 43 (1995) 1685–1689.
[33] J. Crank, The Mathematics of Diffusion, second ed., Clarendon, Oxford, 1975.
[34] R.W. Baker, H.K. Lonsdale, Controlled release: mechanisms and rates, in: A.C. Tanquarry, R.E. Lacey (Eds.), Controlled Release of Biologically Active Agents, Plenum Press, New York, 1974, pp. 15–71.
[35] N.A. Peppas, Mathematical modeling of diffusion process in drug delivery polymeric systems, in: V.F. Smolen (Ed.), Bioavailability and the Pharmacokinetic Control of Drug Response, Wiley, New York, 1980.